Air Pollution, Global Change and Forests in the New Millennium
D.F. Karnosky et al., editors

Chapter 5

Regional scale risk assessment of ozone and forests

G. Gerosa*

DMF, Department of Mathematics and Physics, Università Catolica del Sacro Cuore, via Musei 2, 25121 Brescia, Italy

A. Ballarin-Denti

Department of Mathematics and Physics, Catholic University of Brescia, via Musei 41, 25121 Brescia, Italy

Abstract

The ozone exposure risk for vegetation in Lombardy (Northern Italy) has been assessed by the AOT40 exposure index, based on data taken from the existing local monitoring networks covering 5 growing seasons (1994 to 1998). One-square kilometer exposure maps were obtained by using geostatistic techniques (ordinary kriging) followed by an altitude detrendization of measurement's temporal series to account for the domain's large topographic heterogeneity. Risk areas (Level I maps) were identified using a GIS and overlaying the ozone-critical-level exceedance maps on the distribution maps of forests and sensitive species.

The critical ozone exposure level of 10 000 ppb h, adopted by UN/ECE protocols, is exceeded over the whole Lombardy Territory over the 6-month growing season. The highest risk areas are the northwest pre-alpine and alpine belt, directly impacted by the photo-oxidant plume generated by the Milan urban area. Difficulties met in creating a proper Level II risk assessment for forests in mountain areas have been bypassed by comparing ozone exposures with summer climate features. Soil water availability was assumed not to be a significant modifying factor in the mountains of this region because of the frequent summer rains, whereas the opposite held true for wind ventilation which is generally weak. Field surveys have reported foliar injuries attributable to ozone in different species of forest trees and shrubs, which provide further evidence of potentially phytotoxic ozone levels.

* Corresponding author.

DOI:10.1016/S1474-8177(03)03005-5

1. Introduction

High concentrations of tropospheric ozone and photo-oxidants represent a major environmental concern in most European countries, particularly in the Alpine and Mediterranean regions (Sandroni et al., 1994; Staffelbach et al., 1997), because of their possible negative effects on agricultural and forest ecosystems. The ozone contribution to biological damages and productivity loss, although dependent on species-specific genetic features and environmental conditions, is a function of absorbed dose and, therefore, of the true physiological exposure to this pollutant.

An assessment of photo-oxidants impact on vegetation at regional scale might be based on exposure values obtained from ambient ozone concentrations, aimed at estimating absorbed doses and at predicting plant organisms' responses based on their specific diversity. Although different dose-injury relationships have been reported from studies performed on different grass and tree species in open-top chambers (Fuhrer et al. 1997), it is often difficult to assess damages at territorial scale due to the uncertainty in the determination of pollutant doses realistically absorbed by the vegetation in open field conditions.

The actual uptake at leaf level is in fact influenced by several meteorological factors, such as temperature, precipitation, humidity, evapotranspiration rate and soil water content, all able to affect the stomatal opening and, therefore, the true absorbed dose. The difficulty to collect reliable data on all the necessary parameters at adequate territorial scale and the need to obtain their estimates from model computations make ozone risk assessments for vegetation often limited to the determination of exposures as a first-step approximation.

The consequent land mapping of exposures indexes leads to the so-called Level I assessment as defined in the UN/ECE protocols framework.

2. Methods

In order to identify the risk areas connected to photo-oxidative stress in the forest domains of the Lombardy region in Italy (Fig. 1), Level I maps have been generated on the basis of the AOT40 index—the long-term cumulative exposure index adopted by many ozone risk assessment protocols in Europe. The selected time base covers the vegetative seasons of five years from 1994 to 1998.

The AOT40 (Accumulated exposure Over a Threshold of 40 ppb) is defined as the sum of the differences between the ozone hourly concentrations and the offset threshold of 40 ppb, calculated for all daylight hours (global radiation $\geqslant 50$ W/m^2) of the whole vegetative season which is conventionally set

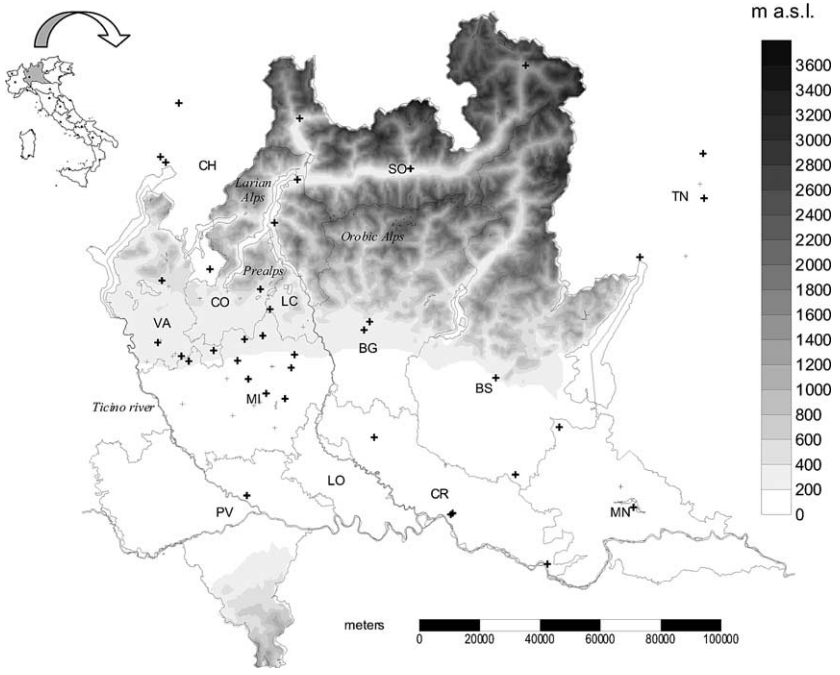

Figure 1. Tropospheric ozone survey network: dislocation of monitoring stations. Stations selected for risk assessment procedure are indicated with bold crosses. Province labels: BG = Bergamo, BS = Brescia, CO = Como, CR = Cremona, LC = Lecco, LO = Lodi, MI = Milano, MN = Mantova, PV = Pavia, SO = Sondrio, VA = Varese, TN = Trento, CH = Switzerland (Canton Ticino).

between April and September for forest vegetation (Kärenlampi and Skärby, 1996).

$$\mathrm{AOT40} := \sum_{[\mathrm{O_3}]_i > 40\ \mathrm{ppb}} \left([\mathrm{O_3}]_i - 40\right). \tag{1}$$

According to several investigations performed on biomass production decrease in forest species (Fuhrer et al., 1997), a critical level of 10 000 ppb h has been adopted by recent UN-ECE protocols and chosen on the assumption that, above it, the appearance of injury symptoms might be expected in the most sensitive species.

2.1. Data collection and mapping procedure

The following procedure has been adopted in the present study for mapping ozone exposure levels: (0) selection of monitoring stations to be accounted for;

(1) raw data collection and database organization; (2) calculation of the AOT40 within the reference period; (3) compensation for missing data; (4) spatial interpolation; (5) generation of final AOT40 maps as average of the five AOT40 maps of the five-year reference period; (6) intersection of AOT40 maps with specific plant receptors maps (vegetation spatial distribution).

Ozone concentration and solar radiation data in the five-year period were obtained as hourly means from the measurements recorded by the regional monitoring stations network and then structured in a proper database. To compensate missing data of solar radiation by some monitoring stations, the mean radiative season for each year was calculated by averaging the available global radiation measurements and the obtained value assigned to stations lacking sufficient data.

The monitoring stations used for AOT40 calculation have been selected according to criteria of (i) sampling efficiency (data capturing $\geqslant 70\%$), (ii) location in rural areas, and (iii) territorial significance. Stations classified as rural, semi-rural or sub-urban (Class A, D and B according to Italian regulations) have been chosen and selected in the listed order. Stations classified as urban (Class C) have been excluded to prevent bias linked to higher ozone-destruction rates by nitrogen oxide (NO) emitted from industrial and transport combustion processes in urban areas. This criterion has been violated only in two cases in order not to leave a whole province domain for each year unrepresented. Lastly, when two or more stations were closer than 5 km, only the station with the highest AOT40f has been chosen to prevent overrepresentation of the area. The configuration of the regional monitoring network (Fig. 1) had not been constant during the reference time domain as far as data sampling efficiency and space location of monitoring stations were concerned. Consequently, the number of stations selected for each year has been varying from 13 to 22, to which 7 more stations were added out of the geographic domain (taken from the monitoring networks of Switzerland and Italian Trento region) in order to improve the system boundary conditions (Table 1).

AOT40 index for crops was calculated over the trimester April 1–June 30, thus modifying the time span suggested by the Kuopio UN-ECE protocol (Kärenlampi and Skärby, 1996). According to this protocol, the critical exposure level for crops has been determined by choosing summer wheat (*Triticum aestivum*) as indicator species. Since wheat is harvested in Italy—differently from what happens in central Europe—before the end of June, we decided to choose accordingly a reference period more representative of the real ozone exposure for wheat.

AOT40 is a cumulative index; this means that any lack of hourly concentration values may produce an underestimate of the overall exposure. The problem has been tackled, under the simplifying assumption of the equi-distribution of the missing data into the different daily hours, by correcting the monthly

Table 1. Ozone monitoring stations. A cross in the last 5 columns indicates the stations which have been selected for the risk assessment procedure

Name	Province or State	Class[a]	Typology	Altitude m a.s.l.	X UTM[b]	Y UTM[b]	'94	'95	'96	'97	'98
Bergamo (S. Giorgio)	BG	C	Urban	249	1 551 800	5 059 540	+	+	+		
Bergamo (Goisis)	BG	A	Rural	249	1 553 660	5 062 285				+	+
Brescia (Broletto)	BS	B	Urban park	149	1 595 495	5 043 695	+	+	+		+
Gambara	BS	D	Semi-rural	51	1 601 980	5 011 530	+	+	+		+
Colico	LC	D	Semi-rural	218	1 529 740	5 109 475				+	
Nibionno	LC	D	Semi-rural	310	1 520 640	5 066 450				+	
Varenna	LC	D	Semi-rural	220	1 522 115	5 095 155	+	+	+	+	
Erba	CO	A	Rural	323	1 517 445	5 073 135		+	+	+	+
Cremona (Libertà)	CR	C	Urban	45	1 581 200	4 998 750	+	+			+
Cremona (Cavour)	CR	B	Sub-urban	45	1 580 520	4 998 300				+	
Crema	CR	B	Sub-urban	79	1 555 170	5 023 910				+	+
Casalmaggiore	CR	B	Semi-rural	23	1 612 575	4 981 835				+	
Mantova (Tè)	MN	B	Sub-urban	18	1 641 120	5 000 670	+	+	+	+	
Castiglione D. Stiviere	MN	B	Semi-rural	116	1 616 488	5 027 282	+	+	+	+	
Agrate Brianza	MI	B	Sub-urban	162	1 527 650	5 047 000					+
Pioltello	MI	D	Sub-urban	123	1 525 610	5 036 750	+	+			
Legnano	MI	B	Sub-urban	199	1 493 695	5 049 200	+	+	+		
Carate Brianza	MI	B	Semi-rural	256	1 518 250	5 057 650		+			+
Meda	MI	B	Sub-urban	221	1 512 230	5 056 500			+	+	
Limbiate	MI	B	Sub-urban	186	1 509 850	5 049 350		+	+	+	
Vimercate	MI	B	Sub-urban	194	1 528 750	5 051 350		+	+	+	
Cormano	MI	B	Sub-urban	146	1 513 450	5 043 250		+			
Milano (Lambro Park)	MI	D	Urban park	122	1 519 350	5 038 500			+	+	
Pavia	PV	B	Urban park	77	1 512 960	5 004 610	+	+	+	+	+
Sondrio	SO	B	Sub-urban	307	1 567 210	5 113 100	+		+	+	
Bormio	SO	B	Semi-rural	1225	1 605 380	5 147 330			+	+	+
Chiavenna	SO	B	Semi-rural	333	1 530 480	5 129 790				+	+
Varese (Vidoletti)	VA	B	Sub-urban	382	1 484 800	5 075 965	+		+	+	+
Saronno	VA	B	Sub-urban	212	1 501 900	5 052 710	+	+	+	+	+
Gallarate	VA	A	Rural	238	1 483 415	5 055 385				+	+
Castellanza	VA	A	Rural	217	1 491 235	5 050 853				+	+
Mendrisio	CH-TI	D	Sub-urban	350	1 496 700	5 077 750	+	+	+	+	+
Bodio	CH-TI	B	Sub-urban	320	1 490 400	5 134 850	+	+	+	+	+
Brione Sopra Minusio	CH-TI	D	Semi-rural	480	1 483 050	5 113 200	+	+	+	+	+
Monte Cimetta	CH-TI	A	Rural, remote	1650	1 481 300	5 115 050	+	+		+	
Trento (Park)	TN	A	Rural	203	1 664 490	5 103 275	+	+	+	+	+
Grumo	TN	D	Semi-rural	228	1 664 160	5 118 126	+			+	+
Riva Del Garda	TN	D	Sub-urban	73	1 643 220	5 083 750	+	+	+	+	+

[a]Letters indicates the station typology according to Italian regulations: A = rural, not directly interested by urban emission sources; B = urban or sub-urban; C = traffic area; D = semi-rural or peripheric sub-urban.

[b]Geographic coordinates are referred to the Mercatore Universal Transvers projection.

"raw" AOT40 by a factor representing the reciprocal of the sampling efficiency for each month

$$\mathrm{AOT40} = \sum_m \frac{\mathrm{AOT40}_{\mathrm{raw}_m} \cdot N_{\mathrm{hours}_m}}{N_{\mathrm{ValidHours}_m}} \tag{2}$$

where N_{hours} is the total number of hours in the considered period, $N_{\mathrm{ValidHours}}$ is the number of hours with valid measurements and the subscript m refers to the mth month.

Maps of spatial distribution for ozone exposure over the whole region were obtained by interpolating single-point AOT40 data on a 1×1 km grid.

2.2. Ozone elevation dependency and geostatistics

Tropospheric ozone concentrations strongly depend on elevation which is in addition a function of precursor levels and solar radiation density. Orographic roughness and clustering of emission sources on valley bottoms lead, in mountain areas, to ozone concentration gradients (and therefore of AOT40 values) even at quite short distances. As a consequence, also the shape of daily cycles of ozone production and depletion is dependent on the station's geographic features and specifically on elevation.

Two different interpolation techniques (Fowler et al., 1995; Loibl et al., 1994), which account for elevation and structure of production-depletion cycles, have been critically evaluated and then applied with some modifications in the present study. Both techniques trace a "basic" trend surface of ozone distribution over the domain. Local variations, due to deviations of measured data from model data, are then interpolated by means of geostatistic techniques such as ordinary kriging (Goovaerts, 1997) or *inverse weighted distance*. The final distribution is obtained by re-assembling the trend surface with the interpolated deviations.

The Loibl technique is based on a model function which takes into account time and elevation dependence of ozone hourly mean concentrations in mountain regions. Its algorithm requires a heavy computational load since more than 4000 hourly maps have to be calculated by *kriging* and then grouped together. Moreover, the *kriging* procedure is by itself only partially automatic since it relies on human expertise in order to choose the correct semi-variogram model, on which the accuracy of kriging depends.

In the present study the Loibl et al. (1994) algorithm was modified with proper parameters to better fit the structure of local ozone data and to calculate over the whole domain the "expected" AOT40 over a six-month growing season as a function of the mean relative altitude of each grid square. The relative altitude was defined as the difference between the mean altitude of the considered grid square and the lowest mean altitude in a 5 km neighborhood. Dif-

ferences between the expected and single-point measured AOT40s were calculated and these residuals krigged over the whole domain after the best fitting of the semi-variogram model. The residuals map was added with the "expected" AOT40 map to obtain the elevation-dependent AOT40 estimate map.

The second technique we considered, originally developed by Fowler et al. (1995) and adopted by the UK Photochemical Oxidants Review Group (1997), is based on the assumption that the structure of the ozone production-depletion cycles and the elevation dependence can be described by one indicator only, the Ratio between the AOT40 measured during daylight hours and that ($AOT40_{mix}$) calculated during the maximal remixing hours (12:00–18:00).

$$\text{Ratio} = \frac{\text{AOT40}}{\text{AOT40}_{\text{mix}}} \tag{3}$$

The assumption originates from the observation that, during the hours of maximal atmosphere remixing, ozone concentrations measured at different elevations are almost similar, in all nearby stations, substantial differences being observed only in the evening and morning hours. Stations located in the plain or near emission sources show Ratio values near 1, whereas remote and more elevated stations, subject to a lower nighttime ozone depletion, have higher values, ranging between 1 and 2.

By means of an analytical relationship between the Ratio and the elevation parameter, Ratio values can therefore be predicted for any point of the territory whose elevation is known. Ratio maps are then obtained by applying this relationship, generally linear, to the terrain digital elevation model of the reference grid. The Ratio parameter, therefore, reflects the basic structural features of ozone distribution. The $AOT40_{mix}$ instead reflects the local characteristics and can be spatially interpolated with ordinary geostatistical techniques.

Finally, AOT40 maps of the whole daylight hours are obtained from $AOT40_{mix}$ and Ratio maps by reversing equation (3)

$$\text{AOT40}(x, y) = \text{AOT40}_{\text{mix}}(x, y) \cdot \text{Ratio}(x, y) \tag{4}$$

and applying equation (4) to every element (x, y) of the grid.

The reliability of this method in Lombardy land conditions is grounded on the elevated thickness of the boundary mixing layer during summertime, which extends to more than 2000 m a.g.l. due to strong thermal atmospheric turbulence. Moreover, $AOT40_{mix}$ is relatively independent from the elevation, thus satisfying the stationary condition requested for the application of the ordinary kriging and allowing the use of this powerful geostatistical technique for interpolation. Differently from the inverse distance weighting method adopted by the UK-PORG investigators, the ordinary kriging approach is also able to produce estimate variance maps allowing researchers to evaluate the estimate's

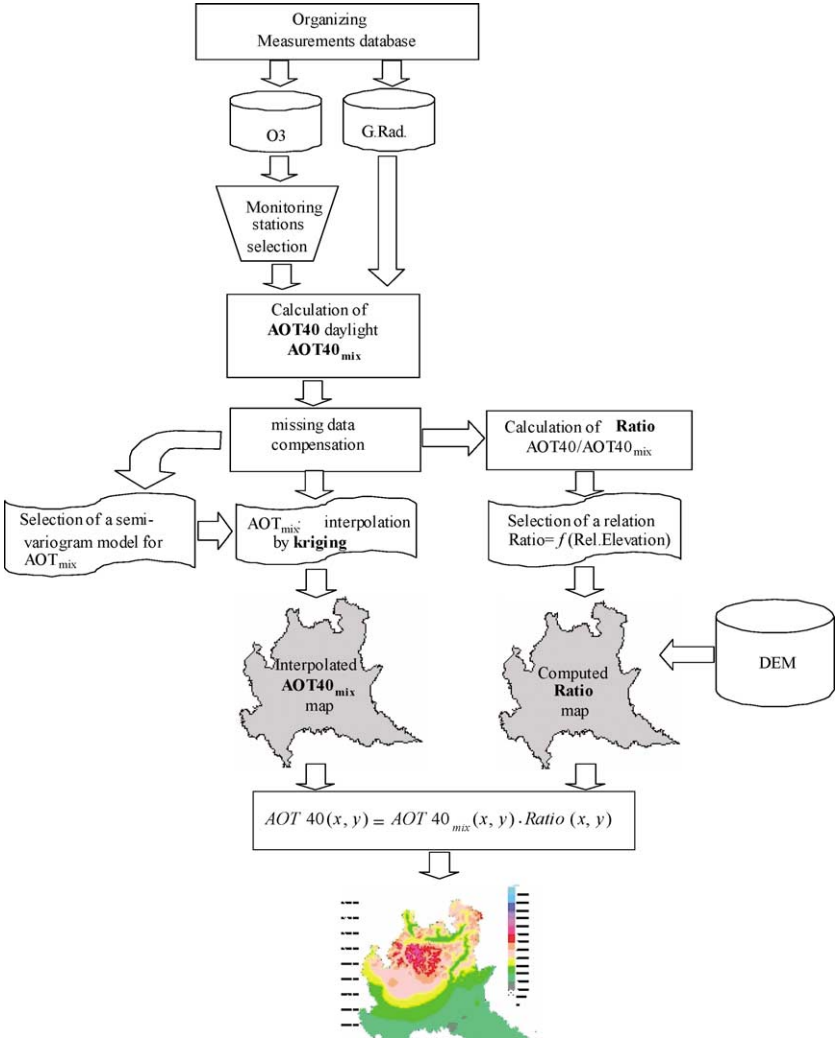

Figure 2. Production of AOT40 maps (outline).

own accuracy. The comprehensive technique scheme is shown in Fig. 2, while details of the semi-variogram functions used in kriging procedure are reported in Table 2.

In order to improve the consistency with the orographic characteristics of the Lombardy territory and to allow an acceptable exposure representation also in higher elevation areas, we decided to modify this technique by replacing

Table 2. Parameters of the semi-variogram functions used in the kriging procedure

$AOT40_{mix}$	Year				
	1998	1997	1996	1995	1994
Semi-variogram model	Linear[a]	Linear	Linear	Linear	Exponential[a]
Range	70.102	87.294	81.343	66.213	16.544
Sill	7.40E+07	1.37E+08	9.59E+07	1.56E+08	8.14E+07
Nugget	0	3.90E+06	0	0	0
RSS	5.37E+16	1.77E+16	4.82E+16	1.87E+17	6.00E+16
Precision (last iteration fit)	1.08E−07	1.11E−10	8.78E−08	1.71E−16	1.73E−07

[a]The function of the linear semi-variogram model is

$$\gamma(h) = \begin{cases} C_0 + C[h], & h < A, \\ C[A], & h \geqslant A \end{cases}$$

and that of the exponential model is $\gamma(h) = C[1 - e^{-h}]$. The parameters C, C_0, A and $C[A]$ represent respectively the scale, the nugget, the range and the sill, while h indicates the spatial lag.

the relative altitude in place of the absolute altitude of the monitoring stations. Consequently, the ratio–altitude function has been changed in terms of Ratio–Relative Altitude (Ratio $= 1.166626 + 0.000682 \cdot$ [Relative Altitude]; $R = 0.88$; $n = 115$; $F = 392$, Significance $p < 0.0001$).

2.3. GIS and geostatistics tools

Finally, to smooth yearly variations of summer ozone levels, five consecutive yearly maps have been averaged according to recommendations put forward by UN/ECE Task Force for mapping (UBA, 1996; Posch et al., 1998).

Ozone risk areas (Level I mapping) have been spotted by means of a GIS (Esra ARC/INFO) and by intertwining exposure exceedances maps with receptors distribution maps obtained from the Territorial Information System of the Lombardy Region at synthesis scale (1 : 250 000).

The procedure of land use classes aggregation adopted to obtain receptors maps as reported in Table 3 and relative notes. CORINE land cover classes are also reported for comparison. Different broadleaf forest managements were not distinguished (high trunk wood and copse). Poplar plantations were aggregated to broadleaf forests.

Receptors maps were calculated as cover percentage for every 1×1 km grid element. The intertwining procedure to obtain Level I maps considered valid only grid elements in which the receptor coverage was at least 1 ha.

Table 3. Receptor classes used in the mapping procedure and their relation with the original land cover classes from the Lombardy Region SIT 250 source. The CORINE Land Cover Classes system is also reported for comparison

Lombardy region SIT 250 land cover classes	CORINE land cover classes	Aggregated land cover classes (receptors)
Water	Closed Urban	Areas not included in the analysis
Barren area	Open Urban	
Quarry	Industrial area	
Industrial and commercial building	Road	
Residential building	Airport	
Big facility and infrastructure	Quarry	
Open space	Waste disposal	
Green Area	Building site	
	Sport area	
	Beach, barren area, etc.	
	Icefield	
	Swamp	
	River	
	Water basin	
	Urban green area	
Sowing-field	Sowing-field	Crops
Rice-field	Rice-field	
Wooden agrarian plantation (orchard, vineyard, etc.)	Vineyard	
	Orchard	
	Olive-grove	
	Stable meadow	
	Annual crop and permanent crop	
	Complex crop system	
	Crop with natural areas	
Pasture lawn	Natural pasture area	Semi-naturals
Uncultivated	Moor and shrubs	
	Trees and shrubs area in evolution	
	Rare vegetation area	
	Fire area	
Broadleaves wood/forest. Copse	Broadleaves forest	Broadleaves forests
Broadleaves wood/forest. High trunk wood	Mixed forest	
Wood plantation (poplar)		
Resinous wood/forest	Conifers forest	Conifers forests

Notes:

– Different broadleaves forest managements were not distinguished (High trunk wood and copse);
– Poplar plantations were aggregated to broadleaves forest;
– The Green Area class has been included in the “area non-included in the analysis” because this class interest quali urban parks, cemeteries, little gardens and green areas with infrastructures;
– Uncultivated area class has been included in the “Semi-natural receptors” because it includes a lot of mountain areas covered by shrubs, bushes, rocks vegetation, etc.).

The GSTAT (Pebesma and Wesseling, 1998, http://www.geog.uu.nl/gstat/) geostatistical tool has been employed in this study. More general tools for different exposure indices computations and for grid choice and manipulation have also been developed (source codes are freely available upon request to the authors).

Surface wind maps were drawn by ordinary kriging starting from hourly measurements obtained by the meteorological monitoring network of the Lombardy Region. Soil water availability was assessed by the Regional Agrometeorological Service (ERSAL) using a simple soil water balance model based on climatic data of the last 30 years (Mariani, 1997; Maracchi et al., 1992), taking into account and properly kriging soil available water capacity, soil depth and covers obtained from the ERSAL pedologic database based on taxonomic units distribution in the region.

Finally, a Digital Elevation Model with 1×1 km grid resolution was generated for the whole domain using data obtained by the Territorial Information System (SIT) of the Lombardy Region and then employed into the mapping procedure.

3. Results and discussion

3.1. Level I risk assessment

The maps obtained by using the two approaches presented in the previous section (UK-PORG and Loibl) provided quite consistent results in terms of proportion of surface exposed to different ozone levels (Table 4) and the exposure spatial patterns turned out to be very similar. By comparison with the UK-PORG "modified" approach, the "modified" Loibl method gave slightly

Table 4. Regional cover (surface percentage) for each forest exposure class (AOT40f computed with three different methods: see references in the text)

Exposure classes AOT40f (ppm.h)	0–5	5–10	10–15	15–20	20–25	25–30	30–35	35–40	40–45	45–50	50–55	55–60	60–65	65–70	70–75
Methods[a]															
UK-PORG (Fowler et al., 1995)	–	–	0.7	33.5	15.9	14.8	20.1	9.5	3.9	1.4	0.3	–	–	–	–
Loibl et al., 1994, modified	–	0.1	1.1	32.8	16.4	12.5	15.3	8.1	5.3	4.2	2.8	1.0	0.2	–	–
UK-PORG modified	–	–	0.1	34.2	18.4	16.6	17.0	7.7	3.4	1.7	0.7	0.2	–	–	–

[a]See references in the text.

higher exposure estimates in the more elevated sites and lower estimates in the valley bottoms. Estimated and measured exposures have been compared selecting the used data set or an independent validation dataset with scattered available measurements (Gerosa et al., 1999; Vecchi and Valli, 1999). In both cases the UK-PORG modified technique showed the lowest residual square's sum (RSS); therefore maps based on this procedure were used for the following risk analysis. The estimate accuracy was quite satisfactory: the kriging's relative standard deviation resulted less than 15% in the most risky areas, with values under 5% in the most densely monitored zones.

The whole region proves to exceed the critical level established for forests (10 000 ppb h), and the most risky areas appear to be located in the northwestern alpine and pre-alpine belt, where exceedances up to 6 times above the critical level have been recorded (Fig. 3). This typical pattern reflects the space distribution of the broad photo-oxidant plume generated by NO_x and VOCs emission within the urban and industrial area located around Milan. In fact, summer breezes push the locally produced ozone from the plain over the mountains, where its lower destruction rate leads to an increase in the background levels.

The distribution of surface areas affected by different ozone exposure classes exhibits a bi-modal feature (Table 4). The largest exposure class lays between 10 000 and 15 000 ppb h (the lower in terms of dose values) and covers 34% of the regional territory; the second most relevant class (between the 30 000 and 35 000 ppb h) covers about 17% of the whole territory. If we consider areas with neither the highest nor the lowest exposure, a major portion of territory (about 60%) shows quite high exposure values ranging between 20 000 and 40 000 ppb h. Fig. 4 shows the percentage of forest areas affected by the different exposure classes.

If we examine forest species distribution (Fig. 5), the most critical conifer forests are located around the northwestern Orobic Alps on both the northern and southern sides. Also, Scotch pine forests in the natural parks located immediately north of Milan are subject to strong stress pressures.

Broadleaved forests (Fig. 5(a)) are spread over the most ozone-risky subalpine belt which stretches from Western Orobic Alps to Larian Alps and Pre-Alps. The distribution area of beech (*Fagus sylvatica*), the forest species for which the critical AOT40f level was established, perfectly matches the core of this area. The diffusion area of black cherry (*Prunus serotina*), alloctone species particularly sensitive to ozone and thus potentially suitable to be used as a bioindicator, covers the Ticino Valleys and the upper western plain. Poplar (*Populus* spp.) cultivation areas in the plain are subject only to a slight exceedance of the critical level, with the exception of those located in the northern belt of Pavia, Lodi and Cremona provinces and the southern side of the Milan province.

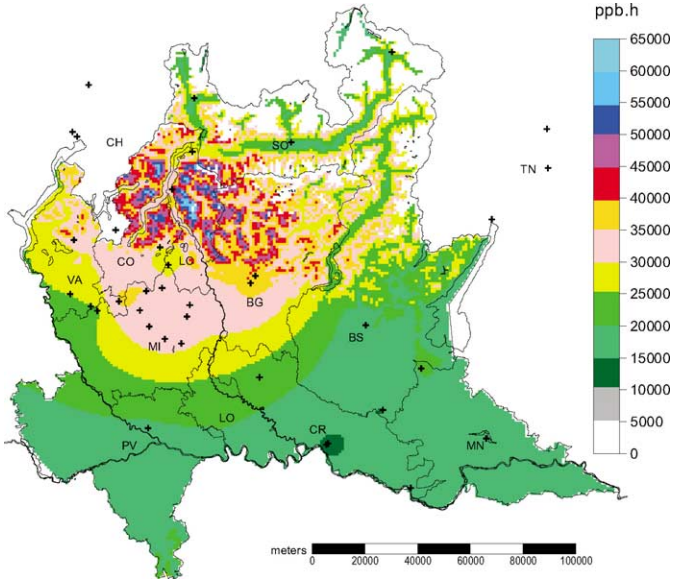

(a) UK-PORG "modified" mapping techniques

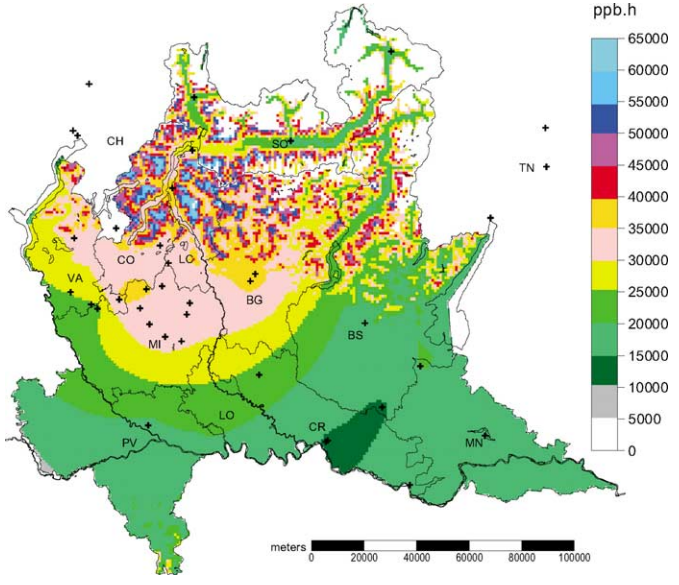

(b) Loibl "modified" mapping techniques

Figure 3. AOT40f in Lombardy. Exposures are expressed in ppmh (April 1st–September 30th, 1994–1998). Crosses indicate ozone monitoring stations. Elevated zones (> 2000 m a.s.l.) are blanked.

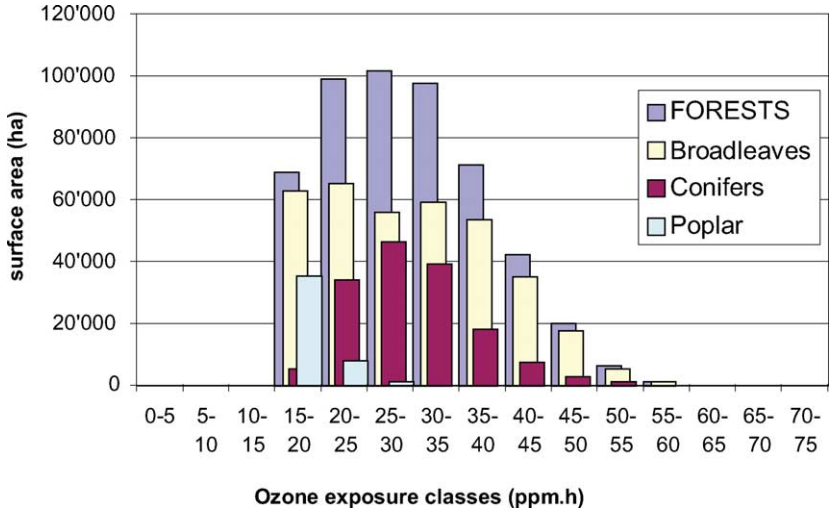

Figure 4. Forests involved in different ozone exposure classes.

3.2. Toward a Level II assessment

Ozone exposure indices offer only a rough approximation of the actual physically absorbed dose which determines the overall plant physiological response. This "real" dose depends on the stomatal conductance that in turn is influenced by a set of meteoclimatic factors able to trigger the complex physiological processes which regulate stomatal opening. Among these environmental physical factors, soil water potential, leaf-to-air water pressure deficit and wind intensity play a major role in influencing ozone uptake by plants (Davidson et al., 1992; Fuhrer, 1995; Grünhage et al., 1997).

Fuhrer (1996a, 1996b), and Posch and Fuhrer (1999) have proposed an easy approach to assess the actual AOT40 for wheat by correcting the calculated AOT40 with multiplicative empirical functions (values from 0 to 1) related to the soil water content, vapor pressure deficit (Emberson et al., 1998).

This approach, developed for ozone risk assessment on crops, is much more difficult to extend to forests because no similar empirical functions have been reported so far for forest populations. We tried, therefore, a semi-quantitative approach to evaluate the weight of these modifying factors on forests in our study case. Ozone exposures maps have been compared with the monthly wind speed and soil water availability distributions of a dry, moist and wet year, obtained from a 30 years historical series respectively as the 10th, 50th, and 90th percentile.

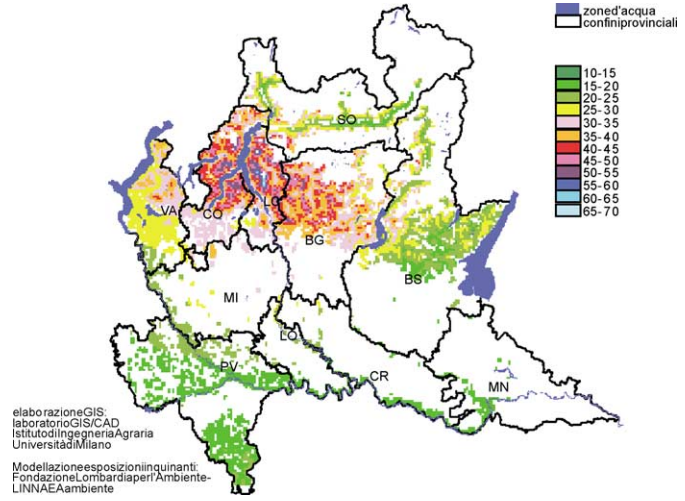

(a) Broadleaf trees

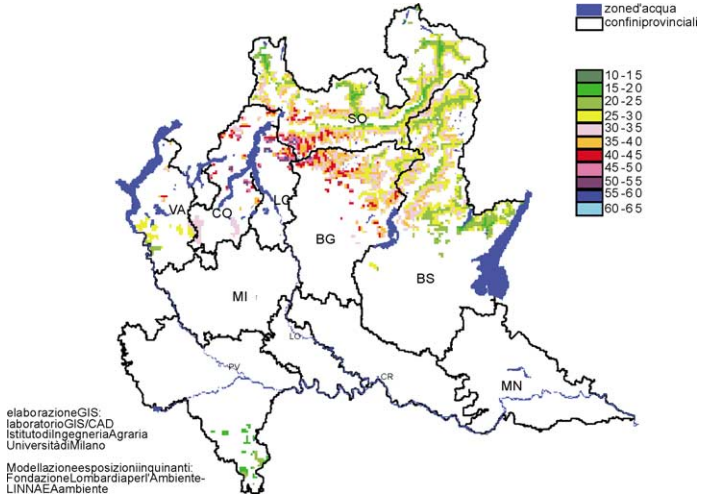

(b) Conifers

Figure 5. Exposures for broadleaf and conifer forests.

The vapor pressure deficit parameter has not been taken into account because of an excess in missing or unreliable data on atmospheric relative humidity, but it is worth mentioning that the summer season in this region is often characterized by elevated humidity.

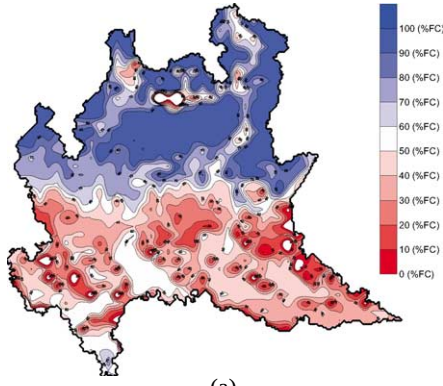

(a)

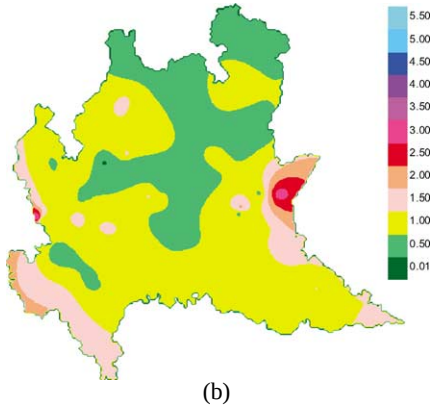

(b)

Figure 6. (a) Soil water content (expressed as % field capacity) in the vegetative semester of the dry year (Q10, $n = 30$ years); (b) Daily mean ventilation (vegetative semester 1994–1998).

During the summer the local insubric climate determines frequent midday rainfalls on the northern hillsides (Maracchi et al., 1992) and hot-and-humid conditions on the plains in the south. As a consequence, the weight of soil water content as the modifying factor for forests—which are located mainly on the hillsides (Fig. 6(a))—may be reduced.

On the other hand, the generally low wind speed seems to play a major role as modifying factor for forests' exposure to ozone (Fig. 6(b)). Because turbulence is reduced in weak ventilation conditions and the ambient ozone concentration surrounding the plants is lowered by dry deposition and/or gas phase reactions.

A significant reduction of the effective AOT40 for forests could be reasonably expected, even though its amount is at present unpredictable because wind measurements are not readily extrapolated in mountain areas—where most forests are located—and only modeling approaches (e.g., MINERVE, Geai, 1987) may help in future developments to reach this goal.

3.3. Survey on observed biological symptoms

Given the high AOT40 levels recorded in the region, both the reduced biological productivity and visible leaf injury symptoms might be expected.

As a qualitative and preliminary check, we searched for data on whether symptomatic ozone leaf responses were reported or not for sensitive species in areas at risk based on the AOT40 exposure maps. We collected and critically reviewed all available ozone leaf injury observations reported independently by different authors for forest and crop species over the region in the same or different years.

Mignanego et al. (1992), Schenone et al. (1995) and the Belgiovine et al. (1999) reported the onset and development of leaf necrosis on tobacco sensitive cultivar Bel-W3 observed in several ozone biomonitoring campaigns; symptoms' extension and AOT40 levels reported in these studies fit well with the estimated AOT40 for plain zones. The same outcome fits the OTC experiments on crops (*Phaseolus vulgaris, Triticum aestivum, Trifolium repens*) performed by the same investigators (Schenone et al., 1992; Fumagalli et al., 1997; Fumagalli et al., 1999)in two sites located in the regional plain aimed to assess the quantitative relation between ozone exposure and yield loss.

Remarkable effects both at biochemical and visible level were reported in *Fagus sylvatica, Picea abies* and *Larix decidua* by Ballarin-Denti et al. (1995, 1998) and Rabotti and Ballarin-Denti (1998) at two forest intensive monitoring plots located in a mountain region at the northern edge of the area subject to the photo-oxidant plume of Milan.

Bussotti et al. (2000) and Cozzi and Ferretti (1999) reported visible leaf symptoms clearly attributable to ozone exposure for different forest native species in a recent survey performed in several sites in the Valtellina Valley in the northern part of the region. They validated the recorded symptoms by comparison with those observed at the Swiss OTC facility of Lattecaldo (Skelly et al., 1998, 1999)—located very close to the Switzerland-Lombardy border, only 50 km north of Milan—and by microscope histology analysis (Gravano, *personal communication*). AOT40 levels at which visible symptoms were observed in non-filtered OTCs well agree with the lower limit of the AOT40s we estimated for the sites where injuries on symptomatic species were reported in field conditions.

Cozzi et al. (1998), Bussotti (*personal communication*) and Gerosa carried out in 1998–2000 other on-field surveys in three broadleaf forest sites located in the highest-risk area (Moggio, Pian dei Resinelli, Forest nursery of Curno) and reported symptoms on a variety of trees, shrubs, vines and herbs species, namely: *Acer pseudoplatanus*, *Ailanthus altissima*, *Carpinus betulus*, *Corylus avellana*, *Fagus sylvatica*, *Fraxinus excelsior*, *Laburnum anagyroides*, *Ostrya carpinifolia*, *Parthenocyssus quinquefolia*, *Populus nigra*, *Prunus avium*, *Rosa spp.*, *Rubus idaeus*, *Rubus ulmifolius*, *Salix alba*, *Salix glabra*, *Sambucus ebulus*, *Sorbus aucuparia*, *Sorbus aria*, *Tilia platyphyllos*, *Ulmus glabra*, *Viburnum lantana*, *Vitis vinifera*; *Alchemilla vulgaris*, *Aquilegia einseleana*, *Atropa belladonna*, *Centaurea nigrescens*, *Euphorbia amygdaloides*, *Mycelis ruralis*, *Rumex alpinum*, *Thalictrum minus*, *Trifolium pratense*, *Valeriana montana*, *Veronica urticifolia.*

On the contrary, they found only few and weak symptoms in other sparse observations carried out in the lowest-risk zones at the end of August in 1998 and 1999.

4. Conclusions

In this study the UN/ECE methodology for assessing ozone risks to forests was applied in a regional context to describe the small-scale distribution of ecosystems at risk. Due to the presence of large emission sources the Lombardy region is one of the most exposed areas in Europe. Some information is available from European-scale mapping exercises, but small-scale information is lacking. Small-scale ozone risk assessment in regions with complex topography needs accurate interpolation methodologies able to account for ozone elevation dependency. Two different techniques have been modified, simplified and made suitable for an appropriate use at regional scale. Both algorithms gave satisfactory results but the mapping algorithm originally developed by Fowler et al. (1995) and modified by introducing the relative height concept was considered to be more reliable. The present study represents the first attempt to draw ozone risk maps in Italy.

Level I risk maps are useful to locate the areas suffering potential ozone risk, but nevertheless are intrinsically limited because these maps are not suitable to predict the real scale of effects on ecosystems. To overcome this limitation a level II evaluation is requested.

Level II ozone risk evaluation is more difficult to achieve for mountain forests than for crops which are cultivated in the plain. To bypass this obstacle, at least in a semi-quantitative way, a contextual analysis of climate features like ventilation, summer rain, potential evapotranspiration, pluviometric deficit or

more detailed soil water balance should be done to better assess Level I calculated exposures. In any case, Level II maps, able to assess the real scale of *effects*, rely on the availability of detailed territorial databases and short-time-resolution meteorological data or their modeled substitutes which are not always easy to obtain at reduced scale.

Maps produced in the present regional case study have proved that ozone exposures in Lombardy are very high both for forests and crops and possibly able to cause visible injury symptoms. Such exposure levels can determine deep modifications in the plant metabolism which can in turn influence both the productivity and stability of natural ecosystems.

Survey campaigns have confirmed the on-field presence of evident foliar injury symptoms in forest populations of the mountainous target of the photo-oxidant plume generated in the lower urban and industrial plain.

Acknowledgements

This project was supported by the Lombardy Region, Department of the Environment, and by the Lombardy Foundation for the Environment as a part of the Regional Air Quality Recovery Plan (PRQA) of the Lombardy Region (2000). The authors are grateful to the Institute of Agricultural Engineering of the University of Milan for the GIS support; to Dr. L. Mariani and M. Russo of the Regional Agrometeorological Service (ERSAL) for soil water balance data and calculations; to Dr. A. Cozzi and M. Ferretti (Linnaea Ambiente of Florence) for their contributions; to Dr. F. Spinazzi for the programming support; to Dr. F. Bussotti, Dr. E. Gravano, Dr. A. Gubertini and the Regional Forest Agency (ARF) for the symptoms validation in the field.

References

Ballarin-Denti, A., Rabotti, G., Tagliaferri, A., Rapella, A., 1995. Novel decline symptoms in an alpine forest system and biochemical indicators of air pollution stress. Life Chem. Rep. 13, 11–119.

Ballarin-Denti, A., Cocucci, S.M., Di-Girolamo, F., 1998. Environmental Pollution and forest stress: A multidisciplinary study on alpine forest ecosystems. Chemosphere 36 (4–5), 1049–1054.

Belgiovine, N., Bergonzi, S., Fumagalli, I., Sormani, L., Mignanego, L., Mietto, S., Ballarin-Denti, A., Brambilla, E., Mazzali, C., 1999. Progetto biennale di Biomonitoraggio della qualità dell'Aria in Provincia di Milano, Final Project Report, Provincia di Milano, Assessorato all'Ambiente, Corso di Porta Vittoria 27, Milano, Italy, p. 70.

Bussotti, F., Mazzali, C., Cozzi, A., Ferretti, M., Gravano, E., Gerosa, G., Ballarin-Denti, A., 2000. Ozone levels and symptoms on vegetation in an alpine valley (North Italy). In: Air Pollution, Global Change and Forests in the New Millennium, 19th International Meeting for Specialists

in Air Pollution Effects on Forest Ecosystems. May 28–31, 2000. Michigan Technological University, Houghton, MI, USA.

Cozzi, A., Cenni, E., Ferretti, M., 1998. Condizione degli alberi nel 1997 nelle Unità Territoriali di Riferimento del lago Maggiore, Oltrepò Pavese, Valchiavenna-Lago di Como, Valtellina, Serio-Brembo, Val Camonica, Lago d'Idro-Chiese e Lago di Garda-Mincio (Livello I). Final Project Report, Vol 1. Regione Lombardia, Azienda Regionale delle Foreste, Milano, Italy.

Cozzi, A., Ferretti, M., 1999. Indagine sui sintomi fogliari visibili attribuibili ad Ozono sulla vegetazione spontanea in Valtellina. Rapporto LINNAEA Ambiente, Firenze.

Davidson, S.R., Ashmore, M.R., Garretty, C., 1992. Effects of ozone and water deficit on the growth and physiology of *Fagus sylvatica*. Forest Ecol. Manag. 51, 187–193.

Emberson, L.D., Ashmore, M.R., Cambridge, H.L., 1998. Development of Methodologies for Mapping Level II Critical Levels of Ozone. DETR Report n. EPG. 1/3/82, Imperial College Centre for Environmental Technology, London.

Fowler, D., Smith, R.I., Coyle, M., Weston, K.J., Davies, T.D., Ashmore, M.R., Brown, M., 1995. Quantifying the fine scale (1 km $\times$ 1 km) exposure and effects of ozone. Part 1. Methodology and application for effects on forests. Water Air Soil Pollut. 85 (3), 1479–1484.

Fuhrer, J., 1995. Critical level for ozone to protect agricultural crops: interaction with water availability. Water Air Soil Pollut. 85, 1355–1360.

Fuhrer, J., 1996a. Key elements in ozone risk analysis. In: Knoflacher, M., Schneider, J., Soja, G. (Eds.), 1996 Exceedance of Critical Loads and Levels, CLRTAP Workshop Report. Vienna, Austria, pp. 1–17.

Fuhrer, J., 1996b. The critical level for effects of ozone on crops and the transfer to mapping. In: Kärenlampi, L., Skärby, L. (Eds.), 1996—Critical Levels for Ozone in Europe: Testing and Finalizing the Concepts, UN-ECE workshop report. Kuopio, Finland, pp. 27–43.

Fuhrer, J., Skärby, L., Ashmore, M.R., 1997. Critical levels for ozone effects on vegetation in Europe. Environ. Pollut. 97, 91–106.

Fumagalli, I., Mignanego, L., Ambrogi, R., 1999. Effetti dell'inquinamento atmosferico sui vegetali: 10 anni di ricerche condotte dall'ENEL. Acqua Aria 10, 109–118.

Fumagalli, I., Mignanego, L., Violini, G., 1997. Effects of tropospheric ozone on white clover plants exposed in open-top chambers or protected by the antioxidant ethylenediurea (EDU). Agronomie 17, 271–281.

Geai, P., 1987. Methode d'interpolation et de reconstitution tridimensionalle d'un champ de vent: le code d'analyse objectie MINERVE. Rep. ARD-AID: E34-E11, EDF, Chatou, France.

Gerosa, G., Spinazzi, F., Ballarin-Denti, A., 1999. Tropospheric ozone in alpine forest sites: Air quality monitoring and statistical data analysis. Water Air Soil Pollut. 116, 345–350.

Goovaerts, P., 1997. Geostatistics for Natural Resources Evaluation. Oxford Univ. Press, New York.

Grünhage, L., Jäger, H.J., Haenel, H.D., Hanewald, K., Krupa, S., 1997. PLATIN (PLant-ATmosphere INteraction) II: Co-occurrence of high ambient ozone concentrations and factor limiting plant absorbed dose. Environ. Pollut. 98, 51–60.

Kärenlampi, L., Skärby, L. (Eds.), 1996. Critical Levels for Ozone in Europe: Testing and Finalizing the Concepts (UN-ECE Workshop Report). Department of Ecology and Environmental Science, University of Kuopio, Kuopio, Finland.

Loibl, W., Winiwarter, W., Kopcsa, A., Züger, J., Baumann, R., 1994. Estimating the spatial distribution of ozone concentrations in complex terrain using a function of elevation and day time and kriging techniques. Atmos. Environ. 28, 2557–2566.

Maracchi, G., Bindi, M., Conese, C., Mariani, L., 1992. Guida Agrometeorologica della Lombardia. ERSAL, Milano, Italy. p. 108.

Mariani, L. (Ed.), 1997. Caratterizzazione Agroclimatica dei Consorzi di Bonifica Lombardi. SIBITeR Project Final Report. ERSAL, Milano Due Palazzo Canova, Segrate (MI), Italy, p. 40.

Mignanego, L., Biondi, G., Schenone, G., 1992. Ozone biomonitoring in northern Italy. Environ. Monit. Assess. 21, 141–159.

Pebesma, E.J., Wesseling, C.G., 1998. Gstat, a program for geostatistical modelling, prediction and simulation. Comput. Geosci. 24 (1), 17–31.

Posch, M., Hetteling, J.-P., de Smet, P.A.M., Downing, R.J. (Eds.), 1998. Calculation and mapping of critical thresholds in Europe: Cordination Center for Effects Status report 1997. RIVM Rep. 259101007. Bilthoven, Netherlands.

Posch, M., Fuhrer, J., 1999. Mapping Level II exceedance of ozone critical levels for crops on a European scale: the use of correction factors. In: Fuhrer, Achermann (Eds.), Critical levels for ozone–Level II. Environmental Documentation N. 115. Swiss Agency for Environment, Forest and Landscape. Bern, Switzerland, pp. 49–53.

Rabotti, G., Ballarin-Denti, A., 1998. Biochemical responses to abiotic stress in beech (*Fagus sylvatica* L.) leaves. Chemosphere 36 (4–5), 871–875.

Sandroni, S., Bacci, P., Boffa, G., Pellegrini, U., Ventura, A., 1994. Tropospheric ozone in the pre-alpine and Alpine Regions. Sci. Total Environ. 156, 169–182.

Schenone, G., Botteschi, G., Fumagalli, I., Montinaro, F., 1992. Effects of ambient air pollution in open-top chambers on bean (*Phaseolus vulgaris* L.). I. effects on growth and yield. New Phytol. 122, 689–697.

Schenone, G., Fumagalli, I., Mignanego, L., Violini, G., 1995. Effects of ambient ozone on bean (*Phaseolus vulgaris* L.): results of an experiment with the antioxidant EDU in the Po plain (Italy) in the 1993 season. Responses of Plants to Air Pollution. Biologic and Economic Aspects. Agricoltura Mediterranea, 104–108.

Skelly, J.M., Innes, J.L., Savage, J.E., Snyder, K.R., Vander-Heyden, D., Zhang, J., Sanz, M.J., 1999. Observation and confirmation of foliar ozone symptoms of native plant species of Switzerland and southern Spain. Water Air Soil Pollut. 116, 227–234.

Skelly, J.M., Innes, J.L., Snyder, K.R., Savage, J.E., Hug, C., Landolt, W., Bleuler, P., 1998. Investigations of ozone induced injury in forests of southern Switzerland: Field surveys and open-top chamber experiments. Chemosphere 36 (4–5), 994–1000.

Staffelbach, T., Neftel, A., Blattner, A., Gut, A., Fahrni, M., Stähelin, J., Prévôt, A., Hering, A., Lehning, M., Neininger, B., Bäumle, M., Kok, G.L., Dommen, J., Hutterli, M., Anklin, M., 1997. Photochemical oxidant formation over Southern Switzerland. I. Results from summer 1994. J. Geophys. Res. 102, 23345–23362.

UBA, 1996. Manual on Methodologies and Criteria for Mapping Critical Levels/Loads and geographical areas where they are exceeded. UN/ECE Convention on Long-Range Transboundari Air Pollution. Federal Environmental Agency (Umweltbundesamt), Texte 71/96, Berlino.

UK-PORG, 1997. Ozone in the United Kingdom. Fourth report of the Photochemical Oxidants Review Group. United Kingdom. ISBN 1-870393-30-9.

Vecchi, R., Valli, G., 1999. Ozone assessment in the southern part of the Alps. Atmos. Environ. 33, 97–109.